

Article

# Live Cell FRET Imaging Reveals Amyloid $\beta$ -Peptide Oligomerization in Hippocampal Neurons

Yang Gao <sup>1</sup>, Stefan Wennmalm <sup>2</sup>, Bengt Winblad <sup>1,3</sup>, Sophia Schedin-Weiss <sup>1</sup> and Lars Tjernberg <sup>1,\*</sup>

<sup>1</sup> Karolinska Institutet, Department of Neurobiology, Care Sciences and Society, Division of Neurogeriatrics, 171 64 Solna, Sweden; yang.gao@ki.se (Y.G.); bengt.winblad@ki.se (B.W.); sophia.schedin.weiss@ki.se (S.S.W.)

<sup>2</sup> Royal Institute of Technology, Department of Applied Physics, Biophysics, SciLifeLab, 171 65 Solna, Sweden; stewart@kth.se

<sup>3</sup> Theme Inflammation and Aging, Karolinska University Hospital, 141 86 Huddinge, Sweden

\* Correspondence: lars.tjernberg@ki.se

**Abstract:** Amyloid  $\beta$ -peptide ( $A\beta$ ) oligomerization is believed to contribute to the neuronal dysfunction in Alzheimer disease (AD). Despite decades of research, many details of  $A\beta$  oligomerization in neurons still need to be revealed. Förster Resonance Energy Transfer (FRET) is a simple but effective way to study molecular interactions. Here we use a confocal microscope with a sensitive Airyscan detector for FRET detection. By live cell FRET imaging, we detect  $A\beta$ 42 oligomerization in primary neurons. The neurons were incubated with fluorescently labelled  $A\beta$ 42 in the cell culture medium for 24 hours.  $A\beta$ 42 were internalized and oligomerized into the lysosomes/late endosomes in a concentration-dependent manner. Both the cellular uptake and intracellular oligomerization of  $A\beta$ 42 were significantly higher than for  $A\beta$ 40. These findings provide a better understanding of  $A\beta$ 42 oligomerization in neurons.

**Keywords:** amyloid  $\beta$ -peptide; oligomerization; aggregation; FRET

**Citation:** Lastname, F.; Lastname, F.;

Lastname, F. Title. *Int. J. Mol. Sci.*

2021, 22, x.

<https://doi.org/10.3390/xxxxx>

## 1. Introduction

Alzheimer disease is the most common cause of dementia, and affects mainly older people [1]. It is estimated to affect over 100 million people worldwide in 2050, and its pathogenesis remains unclear [2]. The aggregation of the amyloid  $\beta$ -peptide ( $A\beta$ ) is believed to play a crucial role in the pathogenesis of Alzheimer disease [3].

$A\beta$  is a 38–43 amino acids peptide cleaved from a transmembrane protein, the  $A\beta$  precursor protein (APP) [4]. It is generated intracellularly and secreted to the extracellular space [5,6]. Among the various  $A\beta$  isoforms,  $A\beta$ 42 is more toxic than other species because it is more prone to aggregate [7].  $A\beta$  oligomers – both intracellular and extracellular – are suggested to impair synaptic function and contribute to cognitive decline during the early stages of AD [8]. Increased intracellular  $A\beta$ 42 has been shown to correlate with AD neuropathology [9,10]. However, more studies on intracellular  $A\beta$  oligomers are needed to understand the pathogenesis in early AD.

Oligomeric  $A\beta$  exist in a dynamic equilibrium, which is sensitive and influenced by the environment and the biophysical analysis can affect the oligomers [11][12]. Several techniques have been used for studying  $A\beta$  oligomerization, such as Thioflavin T assays, SDS polyacrylamide gel electrophoresis (PAGE), and Fluorescence microscopy [13]. However, only a few of them are suitable to use in living cells under physiological conditions.

Förster Resonance Energy Transfer (FRET) is widely used to measure protein interactions in molecular biology. Due to its strong dependence on the distance between the donor and acceptor [14], it has been used for studying cellular  $A\beta$  oligomerization and showed unique capability [15].

Several studies have shown that extracellular  $A\beta$  could be internalized and form aggregates in cells [15,16]. However, some key questions regarding the fate of internalized

A $\beta$  still need to be addressed, such as under what conditions, in which subcellular compartments and to what extent A $\beta$  could oligomerize in neurons.

In this study, we performed live cell FRET imaging to detect A $\beta$ 42 oligomerization in primary neurons, by using a high-resolution confocal microscope with a sensitive Airy-scan detector. We found that monomeric A $\beta$  could be taken up into primary neurons and oligomerize mainly in the lysosomes and/or late endosomes in a concentration-dependent manner.

## 2. Results

### 2.1. Internalized A $\beta$ oligomerizes in lysosomes/late endosomes

Fluorescence Correlation Spectroscopy (FCS), Fluorescence cross-correlation spectroscopy (FCCS), and the combination of FRET and FCS (FRET-FCS) were used to investigate the oligomerization state of A $\beta$  in the cell culture medium. These techniques have been shown capable of detecting A $\beta$  oligomers in solution and FRET-FCS can even detect FRET-active oligomers at fractions below 1% compared to monomers [17]. We prepared 500 nM HiLyte™ Fluor 488 (HF488) A $\beta$ 42 and 500 nM HiLyte™ Fluor 647 (HF647) A $\beta$ 42 in the cell culture medium. The FCCS analysis showed that A $\beta$  aggregation was low in the medium after 24 hours (Figure 1, Figure S1-S3).

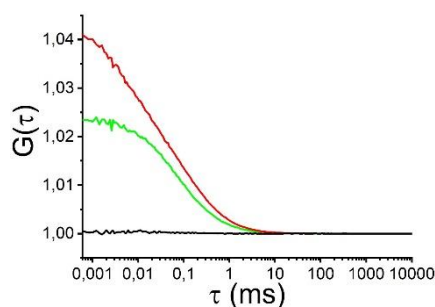


**Figure 1.** FCCS measurements on a sample consisting of 500 nM HF488 A $\beta$ 42 (green) + 500 nM HF647 A $\beta$ 42 (red). Auto- (green and red) and cross-correlation (black) curves were collected in 10 minutes measurement after 24 hours incubation. Laser power: 0.4 % 488 nm and 1.2 % 633 nm. The lack of cross-correlation indicates that a very low number of oligomers, if any, are present. If there were, the black cross-correlation curves would have an amplitude rising above the 1.0-line, like the green and red auto-correlation curve.

Sensitized emission FRET was used to detect A $\beta$  oligomerization in primary neurons (Figure 2a). In this approach, we excited the donor HF488 A $\beta$ 42, which transfers energy directly to the acceptor HF647 A $\beta$ 42 if it is within 10 nm distance, resulting in emission from the acceptor. The emitted light is then detected by a confocal microscope using emission filter for the acceptor. Theoretically, it can be excluded that FRET arises due to the low mean monomer-to-monomer distance of A $\beta$  even at high concentration. Thus, FRET signal in this study indicates A $\beta$  oligomerization.

It should be noted that fluorescence crosstalk from donor, cross excited acceptor, and noises like autofluorescence may interfere with the analysis. To acquire the corrected FRET from crosstalk, spectral bleed-through parameters of the donor and acceptor were determined with cells treated with only HF488 A $\beta$ 42 or only HF647 A $\beta$ 42, respectively. The cell autofluorescence was measured in a non-treated control group. The image analysis was processed using the ImageJ plug-in PixFRET.

Primary hippocampal neurons (21 days in vitro) were incubated in the presence of 500 nM HF488 A $\beta$ 42 and/or 500 nM HF647 A $\beta$ 42 for 24 hours and imaged by a confocal microscope equipped with an Airyscan detector. Both HF488 A $\beta$ 42 and HF647 A $\beta$ 42 were accumulated in the vesicles of the soma (Figure 2b-c). After correction, FRET signal was found in most of the A $\beta$ -containing vesicles (Figure 2d-e).

The corrected FRET can still be affected by the concentration of fluorophores. To get normalized FRET, the corrected FRET value was divided by the square root of the product

of donor and acceptor intensities in each pixel. Figure 2f shows the normalized FRET of the vesicles in the soma of neuron.

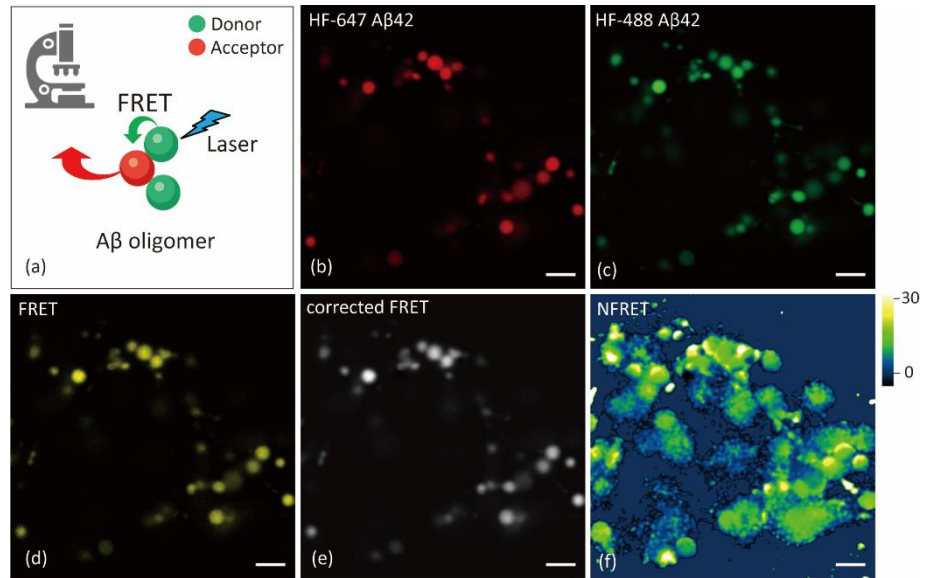


**Figure 2.** FRET analysis to detect aggregated A $\beta$ 42 in primary neurons. (a) Principle of FRET. Equimolar A $\beta$ 42 monomers labeled with HF488 and HF647 are used for oligomerization detection. If the emission of excited donor overlaps with the absorption of the acceptor, energy transfer from donor to ground state acceptor when their distance is 10 nm or less; (b-d) Acceptor channel (640 nm excitation, 650-700 nm emission), donor channel (488 nm excitation, 480-520 nm emission) and FRET channel (488 nm excitation, 650-700 nm emission) of representative FRET image from confocal microscope; (e-f) the corrected FRET and normalized FRET (NFRET) image from ImageJ PixFRET plug-in. Scale bar: 2  $\mu$ m.

Next, to identify the subcellular location where A $\beta$  is accumulated, we used the lysosomal marker SiR-lysosome in neurons that were treated with 1000 nM A $\beta$ 42 for 24h. Most of A $\beta$ -containing vesicles were colocalized with the lysosomal marker (Figure 3). This suggests A $\beta$ 42 is internalized and oligomerized into lysosomes and late endosomes.

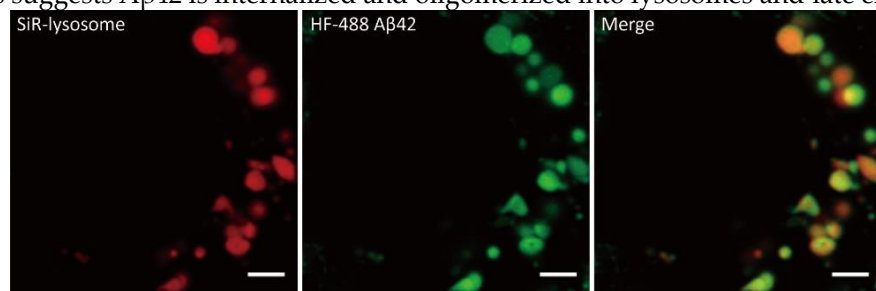


**Figure 3.** Internalized A $\beta$ 42 in primary neurons. DIV 21 neurons were treated with 1000 nM HF488 A $\beta$ 42 (green) for 24h. SiR-lysosome (red) was used to label lysosome and late endosomes. Scale bar: 2  $\mu$ m.

## 2.2. A $\beta$ 42 oligomerization occurs at both surface and vesicles of neurons

A comparison of A $\beta$  oligomerization in vesicles distributed in soma with vesicles in neurites showed no significant differences ( $P > 0.05$ , Fig. 4). The weak A $\beta$  signal on the cell surface was difficult to distinguish from the background, while imaging the vesicles with high intensities in soma without over-saturation. Thus, higher laser power and detector gain were applied to measure the A $\beta$  aggregation on the cell surface. The normalized FRET value of A $\beta$ 42 on the neuron surface or nearabout could be several times higher than in vesicles of soma and neurite. This is consistent in two groups treated with different A $\beta$  concentrations (Figure 5). Similar strong oligomerization was also observed along the neurites although we did not identify if it came from the surface of neurites .

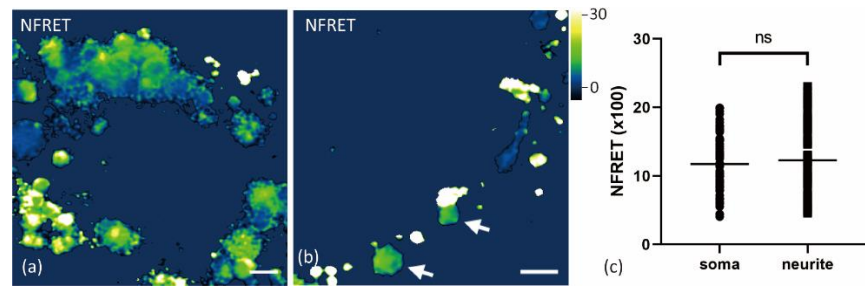


**Figure 4.** Comparison of FRET between A $\beta$  vesicles in soma and neurites. Primary neurons were treated with 500 nM HF488 A $\beta$ 42 and 500 nM HF647 A $\beta$ 42 for 24h. (a) normalized FRET (NFRET) image of A $\beta$  vesicles in soma; (b) NFRET image of A $\beta$  vesicles (white arrow) in neurites; (c) NFRET value of 63 vesicles in soma and 64 vesicles in neurite were compared using Mann-Whitney test ( $P > 0.05$ ). Scale bar: 2  $\mu$ m.

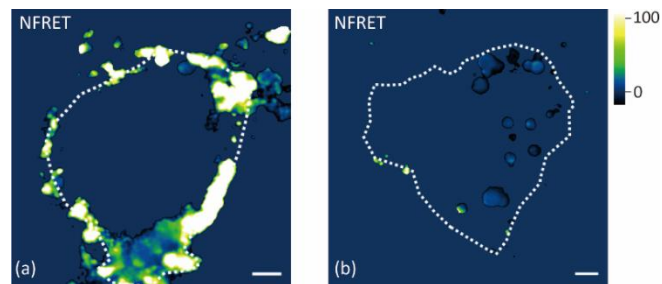


**Figure 5.** Normalized FRET (NFRET) images of A $\beta$  on the cell surface. Primary neurons were treated with 500 nM HF488 A $\beta$ 42 + 500 nM HF647 A $\beta$ 42 (a) or 125 nM HF488 A $\beta$ 42 + 125 nM HF647 A $\beta$ 42 (b) for 24h. The cell bodies of neurons are outlined with the white dashed lines. Scale bar: 2  $\mu$ m.

### 2.3. Internalized A $\beta$ 42 oligomerization in soma is concentration-dependent

To further confirm the association between A $\beta$ 42 oligomerization and concentration in soma, primary neurons were treated with three different A $\beta$  concentrations (HF488 A $\beta$ 42 and HF647 A $\beta$ 42 at 1:1 ratio; 250, 500 and 1000 nM A $\beta$  in total) for 24h. As shown in Figure 6, A $\beta$  oligomerization occurred in all the three groups, and increased with extracellular A $\beta$  concentration. We also found a negative correlation between the diameter of the A $\beta$  vesicles and the normalized FRET level in two cell groups treated with higher A $\beta$  concentration. The smaller vesicles tend to present higher oligomerization level in cells treated with 1000 nM A $\beta$ 42 ( $r = -0.46$ ,  $P < 0.05$ ) and 500 nM A $\beta$ 42 ( $r = -0.28$ ,  $P < 0.05$ ). There was no significant correlation in 250 nM group ( $r = 0.23$ ,  $P > 0.05$ ).

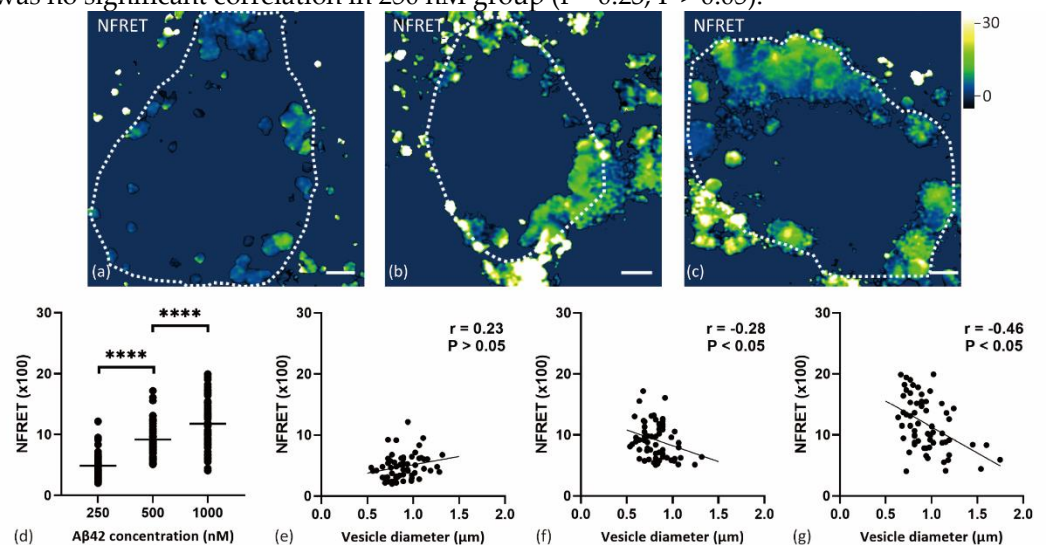


**Figure 6.** Internalized A $\beta$ 42 oligomerization in neuronal soma. (a-c) normalized FRET (NFRET) image of vesicles in soma. Primary neurons were treated with 250 nM A $\beta$ 42 (a) or 500 nM A $\beta$ 42 (b) or 1000 nM A $\beta$ 42 (c) for 24h; (d) NFRET values of 63 vesicles from each group were calculated and compared using ANOVA test ( $P < 0.0001$ ); (e-g) Pearson correlation of A $\beta$  vesicle size and NFRET values in neurons treated with 250 nM A $\beta$ 42 (e) or 500 nM A $\beta$ 42 (f) or 1000 nM A $\beta$ 42 (g) for 24h.

#### 2.4. Internalized A $\beta$ 42 oligomerizes in neurons with higher efficiency than A $\beta$ 40

Finally, we treated primary neurons with fluorescently labeled A $\beta$ 40, and compared the polymerization of internalized A $\beta$ 40 and A $\beta$ 42. Confocal image analysis showed that more A $\beta$ 42 were taken up into neurons than A $\beta$ 40 using the same concentrations for 24 hours, and the A $\beta$ 42 oligomerization level was significantly higher as well (Figure S4).

Because the difference of oligomerization could be due to different A $\beta$  concentrations in vesicles, we then compared vesicles with similar intensity of A $\beta$ 42 and A $\beta$ 40. A $\beta$  concentration in vesicles of cells treated with 1000 nM A $\beta$ 40 for 24 hours was comparable to some of those treated with 250 nM A $\beta$ 42 (Figure 7 a-b). Therefore, we selected vesicles with similar A $\beta$  concentration from these two groups and compared their normalized FRET level. A $\beta$ 42 treatment was found to induce more oligomerization than A $\beta$ 40, under similar A $\beta$  concentrations in vesicles (Figure 7 c-f).

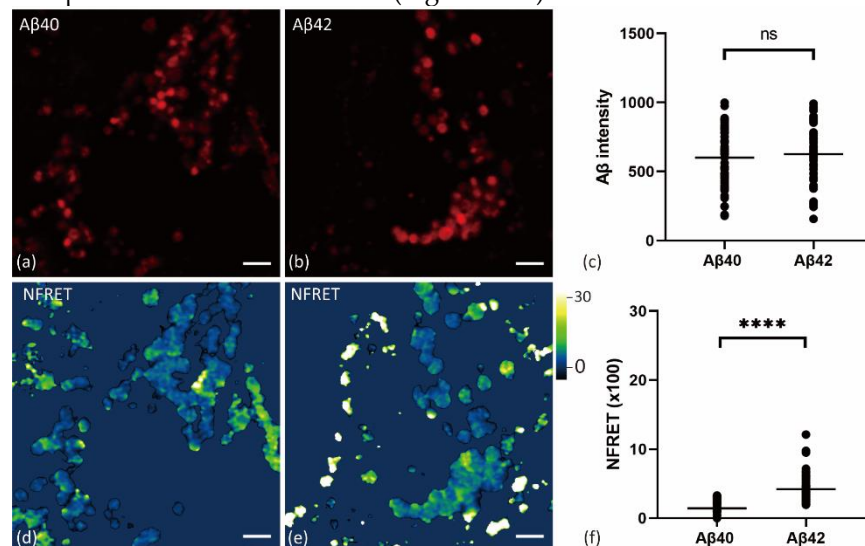


**Figure 7.** FRET images of neurons treated with A $\beta$ 40 or A $\beta$ 42. Primary neurons were treated with 1:1 mixed 1000 nM A $\beta$ 40 (a, d) or 250 nM A $\beta$ 42 (b, e) for 24h. (a-b) Confocal images of A $\beta$  vesicles (HF647) in primary neurons, the same acquisition and display settings were used for both groups; (c) A $\beta$  intensity (HF647) of selected vesicles in neurons treated with 1000 nM A $\beta$ 40 (N=65) and 250 nM A $\beta$ 42 (N=54) were compared using Mann-Whitney test ( $P > 0.05$ ); (d-e) normalized FRET (NFRET) images of A $\beta$  vesicles in primary neurons; (f) NFRET values of selected A $\beta$  vesicles in neuron treated with A $\beta$ 40 and A $\beta$ 42 were compared using Mann-Whitney test ( $P < 0.0001$ ).

Figure 8 shows the scatter plot of normalized FRET values and A $\beta$  concentration in the vesicles of cells treated with different A $\beta$  concentrations. The aggregation of both A $\beta$ 42 and A $\beta$ 40 showed strong trends to increase with their concentrations in vesicles. Despite lower external concentration, A $\beta$ 42 still aggregated to a higher extent than A $\beta$ 40.

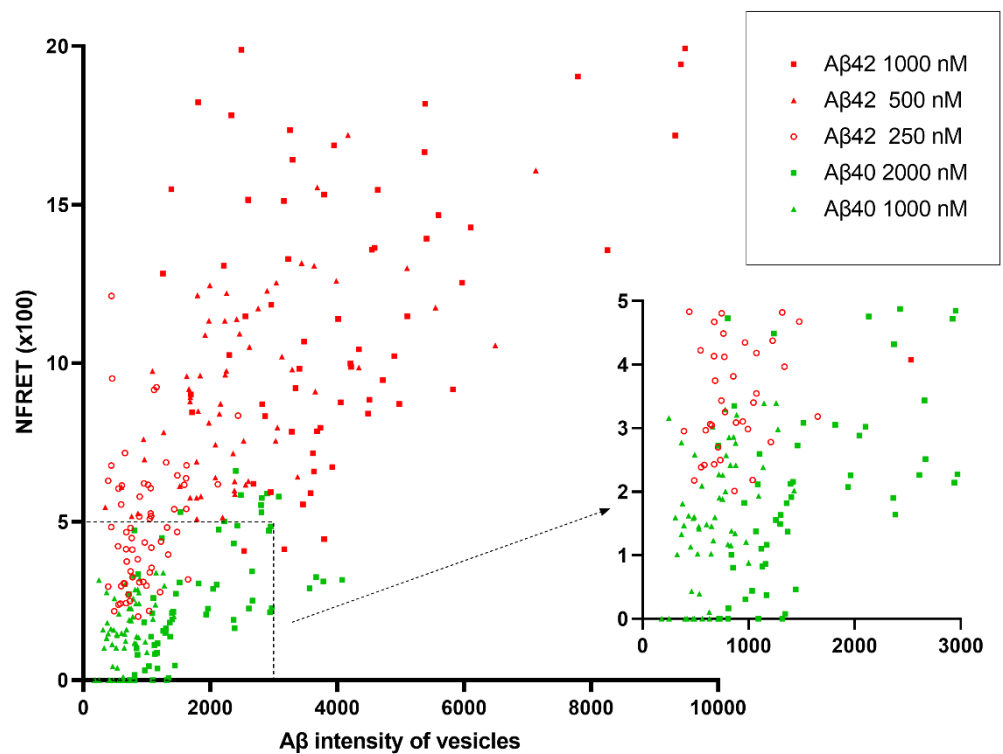


**Figure 8.** Scatter plot of normalized FRET (NFRET) and A $\beta$  intensity (HF647) in vesicles of neuronal soma. Primary neurons were treated with different concentrations of A $\beta$ 40 (green) or A $\beta$ 42 (red) for 24 hours. The right graph shows enlarged details in the dashed box.

### 3. Discussion

A $\beta$  aggregation is thought to have a crucial role in the progression of AD. However, the detection of A $\beta$  oligomers is challenging due to lacking stability and being easily influenced during analysis [18]. FRET has been used to measure molecular distances at the nanoscale for a long time. Here by measuring FRET with a confocal microscope with an Airyscan unit, we confirm that extracellular monomeric A $\beta$  could be internalized into the murine hippocampal neurons to form oligomers in lysosomes and/or late endosomes.

It has been suggested that intraneuronal A $\beta$  accumulation could be an early event in the pathogenesis of AD [4]. In this study, extracellular A $\beta$  is taken up by neurons and oligomerize intracellularly, making it a possible source of intraneuronal A $\beta$  aggregation. We observed strong A $\beta$  oligomerization occurred in primary neurons treated with only 250 nM A $\beta$ 42 for 24 hours. Previously, Hu et al. did not detect A $\beta$  aggregation in SHSY5Y cells treated with 500 nM A $\beta$ 42 or below for 5 days, using agarose gel electrophoresis-SDS [16]. This might be due to the cellular uptake difference of A $\beta$ , or because A $\beta$  oligomers are SDS-unstable species and this analysis could result in disassembly of oligomers [13].

In our study, A $\beta$  in neurons aggregates in a concentration-dependent manner. This is consistent with previous study in SHSY5Y cells and in buffers [16,19]. Besides, the size of A $\beta$  vesicles also showed a significant negative relation with aggregation in cells with 24 hours treatment of higher A $\beta$  concentration, but not in lower concentration. We suggest that cells with lower A $\beta$  concentration treatment could be at an earlier stage of uptake at 24 hours, compared with those with high concentrations.

The A $\beta$  oligomer distribution in neuron is also interesting. It is reported that more lysosomes located in soma than in neurites [20]. However, the oligomerization level in lysosomes/late endosomes of soma and neurites seems similar. We also identified the strongest normalized FRET signal on the neuron surface based on the following consideration. First, the fluorescence on the cell surface lacks movement during imaging, different from those in the cellular organelles. Secondly, such distinctly high normalized FRET was

observed only on the cell border and along neurites, but not in soma. Besides, it has been reported that A $\beta$  form oligomers on lipid rafts in the cell membrane [21].

Regarding intraneuronal A $\beta$ 42 aggregation, another question is where this progress begins. First, we detected only little A $\beta$ 42 oligomerization at a 1000 nM concentration in the cell culture medium. Secondly, we noticed high A $\beta$  oligomerization on the surface of neuron. The values of normalized FRET are several times higher than in the soma. The normalized FRET can be affected by the distance-dependent FRET efficiency and the ratio of "FRET" donor-acceptors to all the donors and acceptors [22]. In this study, such a large difference in the normalized FRET between soma and membrane cannot be explained by the FRET efficiency. Thus, we infer that lysosomes/late endosomes in soma contain non-FRET monomeric A $\beta$ 42. The concentration of A $\beta$ 42 in those vesicles is much higher than in extracellular space [16]. Low pH in the lysosomes/late endosomes might promote A $\beta$  aggregation [19,23]. Considering the high concentration and low pH, A $\beta$  monomers in these vesicles are more likely to be taken up extracellularly rather than depolymerized from oligomers. We suggest that at least part of A $\beta$  is internalized in the monomeric form, then aggregates in the late endosomes/lysosomes. However, it is possible that part of A $\beta$  oligomerize at the cell surface before entering late endosomes/lysosomes. It is also possible that oligomers that formed in neurons are released and then re-internalized to the endo-lysosomal system.

Compared with A $\beta$ 42, A $\beta$ 40 is less prone to form fibrils [24]. In the present study, A $\beta$ 42 aggregation dominance in neurons is partly owing to the cellular uptake preference, which results in high A $\beta$ 42 concentration in vesicles. Under similar concentrations in vesicles, A $\beta$ 42 still oligomerizes more than A $\beta$ 40, however the difference is less than we expected. Although normally A $\beta$ 42 is present at lower concentrations than A $\beta$ 40 [25], it can induce more oligomers due to the enhanced cellular uptake and its strong aggregation tendency. This novel finding is in line with our previous finding showing elevated levels of A $\beta$ 42 in neurons at risk in AD brain [9]. Thus, we hypothesize that A $\beta$ 42 accumulation in neurons by enhanced uptake is an early pathogenic event in AD, and that inhibition of this process could be a pharmacological strategy for treating AD.

In this study, we chose sensitized emission FRET for several reasons. It is simple, nondestructive, suitable for live imaging, and our study also fit the stoichiometry of 1:1 donor and acceptor. The fast and sensitive Airyscan unit allowed us to detect FRET signal in moving vesicles, but it also detected unwanted autofluorescence. To minimize the caused false positive FRET, autofluorescence was measured from the non-treated vesicles that present the fluorescence. However, detected autofluorescence existed only in part of vesicles, so background subtraction from the whole image might underestimate the FRET of those compartments with less autofluorescence, or even result in false negative values. In addition, although the bleed-through parameters were determined carefully, it was still difficult to measure accurate FRET data quantitatively with sensitized emission FRET, especially when the FRET signal was weak. This limits the use of sensitized emission FRET in some applications, like to determine the lowest A $\beta$  concentration or the earliest timepoint to aggregate. Nevertheless, live cell FRET imaging can provide in situ detection with almost no intervention, making it a robust and unique technique for oligomerization measurement, when designed properly and conducted under controlled conditions.

In summary, our study suggests that A $\beta$ 42 monomer can be internalized in neurons and oligomerize in the late endosome/lysosomes with high efficiency. In such a way, A $\beta$ 42 oligomers might accumulate gradually in neurons in decades of lifetime, and cause the neuronal dysfunction.

#### 4. Materials and Methods

##### 4.1. Synthetic human A $\beta$ Peptide and Preparation

A $\beta$  (1–40) and A $\beta$  (1–42) peptides, labeled with HiLyte™ Fluor 488 or HiLyte™ Fluor 647 at the N-termini, were purchased from AnaSpec (CA, USA). A $\beta$  peptides were

reconstituted by adding 40-50  $\mu$ l 1% NH<sub>4</sub>OH to 0.1 mg dry peptide and diluted to 1 mg/ml with PBS, then aliquoted and stored at -20°C.

#### 4.2. Primary neuron culture

Hippocampal neurons were isolated from the hippocampi of E16.5 C57/BL6 mice mouse embryo brain, seeded on the inner 10-mm microwell of poly-d-lysine-coated glass-bottom of P35G-1.5-10-C culture dishes (MatTek Corporation), as described previously [26]. Cortical neurons were seeded at the pre-coated edges of the plate as a support layer. Both hippocampal and cortical neurons were grown in selective Neurobasal medium containing 2% B27 (Invitrogen) and 1% L-glutamine (Invitrogen) at 37 °C in a cell incubator (humidified, 5% CO<sub>2</sub>), and cultured for 21 days in vitro (DIV).

#### 4.3. Lysosomes/late endosomes labelling in live cell imaging

Lysosomes/late endosomes were labelled using SiR-Lysosome (Spirochrome AG). Primary neurons were treated with 1000 nM SiR-Lysosome at 37°C, 5% CO<sub>2</sub>, 0.5 hour before imaging.

#### 4.4. Confocal microscope and FRET measurements

Confocal and FRET images were acquired by Zeiss LSM 800 confocal microscope with Airyscan detector, using a Plan-Apochromat 63x/1.4 oil-immersion objective and the 488 and 640 nm laser lines as excitation source. For FRET measurements, the laser power and detector gain for all channels were fixed through the whole experiment. Each channel was subsequently scanned by a 32-channel gallium arsenide phosphide photomultiplier tube (GaAsP-PMT) Airyscan detector with a scan speed of 2.2  $\mu$ s/pixel. 5–10 images were captured per cell culture dish.

The cells were incubated with either HF488 A $\beta$  or HF647 A $\beta$ , or an equimolar mixture of them. The donor control group were imaged sequentially in donor emission (488 nm excitation, 480-520 nm emission) and donor bleed-through (488 nm excitation, 650-700 nm emission). The acceptor control group included acceptor emission (640 nm excitation, 650-700 nm emission) and acceptor crosstalk (488 nm excitation, 650-700 nm emission). The FRET group contained three image sets: donor emission, acceptor emission, and FRET channel (488 nm excitation, 650-700 nm emission). The non-treated neurons group that used to detect the cell autofluorescence and background shared the same setting with FRET group.

FRET analysis was performed using ImageJ plug-in PixFRET as previously described [27]. Concisely, spectral bleed-through were first determined in each image acquired from donor control group and acceptor control group, by using a constant model in PixFRET. A Gaussian blur value of 2.0 was applied during the determination. By applying PixFRET computation, the original FRET images were then corrected from the spectral bleed-through and generated the FRET and normalized FRET image. "FRET/sqrt (Donor\*Acceptor)" was selected as output of normalized FRET, in which values for each pixel were divided by the square root of donor and acceptor intensities from same pixels. Gaussian blur (2.0) and threshold (1.0) values were set for all the images. To clearly distinguish the low and high values, normalized FRET images were displayed in a lookup table "Green Fire Blue". For comparison, the negative normalized FRET values will be set to 0. The quantification of normalized FRET values and A $\beta$  intensity in vesicles were measured with ImageJ. A $\beta$  intensity is calculated with HF647 A $\beta$  because acceptor emission is not affected by FRET.

FCS, FCCS and FCS-FRET measurements were using a Zeiss 780 confocal laser scanning microscope equipped for FCS, with a Zeiss water immersion objective, C-Apochromat 40x/1.2 NA. The measurements have been described previously [17]. In this study, FRET-FCS was performed on the cell-free neuronal culture medium with 24 hours treatment of 500 nM HF488 A $\beta$ 42 and 500 nM HF647 A $\beta$ 42. The diffusion time ( $\tau$ ) refers to the mean time of fluorescent particles passing through the detection focus.

#### 4.5. Statistics

Statistical tests were using the GraphPad Prism 8 software. Normality was assessed using D'Agostino & Pearson test. Non-parametric Mann–Whitney test was used for the data were not normally distributed. One-way ANOVA was used for comparison of three groups. Correlation analysis were tested by Pearson method. When the p value was less than 0.0001, it is stated as “\*\*\*\*”, and “\*” for  $p < 0.05$ . If the p was greater than 0.05, it is stated as  $p > 0.05$  or “ns”.

**Supplementary Materials:** The following are available online at [www.mdpi.com/xxx/s1](http://www.mdpi.com/xxx/s1).

**Author Contributions:** Conceptualization, Y.G., S.S-W., and L.T.; methodology, Y.G., S.W., S.S-W., and L.T.; formal analysis, Y.G. and S.W.; writing—original draft preparation, Y.G., and S.W.; writing—review and editing, Y.G., S.W., S.S-W., and L.T.; visualization, Y.G. and S.W.; supervision, B.W., S.S-W., and L.T.; funding acquisition, S.S-W., B.W., and L.T. All authors have read and agreed to the published version of the manuscript.

**Funding:** This work was supported by grants from Margaretha af Ugglas’ foundation (B.W., S.S-W.), Swedish Alzheimer foundation (L.T. and S.S-W.), Swedish Research Council (L.T.), China Scholarship Council, Stiftelsen för Gamla Tjänarinnor, Gun and Bertil Stohnes Foundation.

**Institutional Review Board Statement:** The ethical permit is approved by Linköping ethical committee (2018/01/25). No experiments are performed on live animals.

**Data Availability Statement:** The data presented in this study are available on request from the corresponding author.

**Acknowledgments:** We acknowledge help from Sylvie Le Guyader and Gabriela Imreh from the Live Cell Imaging facility, Karolinska Institutet, Sweden, supported by grants from the Knut and Alice Wallenberg Foundation, the Swedish Research Council, the Centre for Innovative Medicine and the Jonasson center at the Royal Institute of Technology, Sweden.

**Conflicts of Interest:** The authors declare no conflict of interest.

## References

- Ballard, C.; Gauthier, S.; Corbett, A.; Brayne, C.; Aarsland, D.; Jones, E. Alzheimer’s Disease. *Lancet Lond. Engl.* 2011, 377, 1019–1031, doi:10.1016/S0140-6736(10)61349-9.
- 2020 Alzheimer’s Disease Facts and Figures. *Alzheimers Dement.* 2020, 16, 391–460, doi:https://doi.org/10.1002/alz.12068.
- Viola, K.L.; Klein, W.L. Amyloid  $\beta$  Oligomers in Alzheimer’s Disease Pathogenesis, Treatment, and Diagnosis. *Acta Neuropathol. (Berl.)* 2015, 129, 183–206, doi:10.1007/s00401-015-1386-3.
- LaFerla, F.M.; Green, K.N.; Oddo, S. Intracellular Amyloid- $\beta$  in Alzheimer’s Disease. *Nat. Rev. Neurosci.* 2007, 8, 499–509, doi:10.1038/nrn2168.
- Turner, R.S.; Suzuki, N.; Chyung, A.S.; Younkin, S.G.; Lee, V.M. Amyloids Beta40 and Beta42 Are Generated Intracellularly in Cultured Human Neurons and Their Secretion Increases with Maturation. *J. Biol. Chem.* 1996, 271, 8966–8970, doi:10.1074/jbc.271.15.8966.
- Tienari, P.J.; Ida, N.; Ikonen, E.; Simons, M.; Weidemann, A.; Multhaup, G.; Masters, C.L.; Dotti, C.G.; Beyreuther, K. Intracellular and Secreted Alzheimer Beta-Amyloid Species Are Generated by Distinct Mechanisms in Cultured Hippocampal Neurons. *Proc. Natl. Acad. Sci. U. S. A.* 1997, 94, 4125–4130, doi:10.1073/pnas.94.8.4125.
- Walsh, D.M.; Selkoe, D.J. A $\beta$  Oligomers – a Decade of Discovery. *J. Neurochem.* 2007, 101, 1172–1184, doi:https://doi.org/10.1111/j.1471-4159.2006.04426.x.
- Karisetty, B.C.; Bhatnagar, A.; Armour, E.M.; Beaver, M.; Zhang, H.; Elefant, F. Amyloid- $\beta$  Peptide Impact on Synaptic Function and Neuroepigenetic Gene Control Reveal New Therapeutic Strategies for Alzheimer’s Disease. *Front. Mol. Neurosci.* 2020, 13, doi:10.3389/fnmol.2020.577622.
- Hashimoto, M.; Bogdanovic, N.; Volkmann, I.; Aoki, M.; Winblad, B.; Tjernberg, L.O. Analysis of Microdissected Human Neurons by a Sensitive ELISA Reveals a Correlation between Elevated Intracellular Concentrations of Abeta42 and Alzheimer’s Disease Neuropathology. *Acta Neuropathol. (Berl.)* 2010, 119, 543–554, doi:10.1007/s00401-010-0661-6.
- Aoki, M.; Volkmann, I.; Tjernberg, L.O.; Winblad, B.; Bogdanovic, N. Amyloid  $\beta$ -Peptide Levels in Laser Capture Microdissected Cornu Ammonis 1 Pyramidal Neurons of Alzheimer’s Brain. *NeuroReport* 2008, 19, 1085–1089, doi:10.1097/WNR.0b013e328302c858.
- Nag, S.; Sarkar, B.; Bandyopadhyay, A.; Sahoo, B.; Sreenivasan, V.K.A.; Kombrabail, M.; Muralidharan, C.; Maiti, S. Nature of the Amyloid- $\beta$  Monomer and the Monomer-Oligomer Equilibrium. *J. Biol. Chem.* 2011, 286, 13827–13833, doi:10.1074/jbc.M110.199885.

12. 12. Hayden, E.Y.; Teplow, D.B. Amyloid  $\beta$ -Protein Oligomers and Alzheimer's Disease. *Alzheimers Res. Ther.* 2013, 5, 60, doi:10.1186/alzrt226.
13. 13. Bruggink, K.A.; Müller, M.; Kuiperij, H.B.; Verbeek, M.M. Methods for Analysis of Amyloid- $\beta$  Aggregates. *J. Alzheimers Dis.* 2012, 28, 735–758, doi:10.3233/JAD-2011-111421.
14. 14. Algar, W.R.; Hildebrandt, N.; Vogel, S.S.; Medintz, I.L. FRET as a Biomolecular Research Tool — Understanding Its Potential While Avoiding Pitfalls. *Nat. Methods* 2019, 16, 815–829, doi:10.1038/s41592-019-0530-8.
15. 15. Wesén, E.; Gallud, A.; Paul, A.; Lindberg, D.J.; Malmberg, P.; Esbjörner, E.K. Cell Surface Proteoglycan-Mediated Uptake and Accumulation of the Alzheimer's Disease Peptide A $\beta$ (1–42). *Biochim. Biophys. Acta BBA - Biomembr.* 2018, 1860, 2204–2214, doi:10.1016/j.bbamem.2018.08.010.
16. 16. Hu, X.; Crick, S.L.; Bu, G.; Frieden, C.; Pappu, R.V.; Lee, J.-M. Amyloid Seeds Formed by Cellular Uptake, Concentration, and Aggregation of the Amyloid-Beta Peptide. *Proc. Natl. Acad. Sci.* 2009, 106, 20324–20329, doi:10.1073/pnas.0911281106.
17. 17. Wennmalm, S.; Chmyrov, V.; Widengren, J.; Tjernberg, L. Highly Sensitive FRET-FCS Detects Amyloid  $\beta$ -Peptide Oligomers in Solution at Physiological Concentrations. *Anal. Chem.* 2015, 87, 11700–11705, doi:10.1021/acs.analchem.5b02630.
18. 18. Mroccko, B.; Groblewska, M.; Litman-Zawadzka, A.; Kornhuber, J.; Lewczuk, P. Amyloid  $\beta$  Oligomers (A $\beta$ Os) in Alzheimer's Disease. *J. Neural Transm.* 2018, 125, 177–191, doi:10.1007/s00702-017-1820-x.
19. 19. Burdick, D.; Soreghan, B.; Kwon, M.; Kosmoski, J.; Knauer, M.; Henschen, A.; Yates, J.; Cotman, C.; Glabe, C. Assembly and Aggregation Properties of Synthetic Alzheimer's A4/Beta Amyloid Peptide Analogs. *J. Biol. Chem.* 1992, 267, 546–554, doi:10.1016/S0021-9258(18)48529-8.
20. 20. Kulkarni, V.V.; Maday, S. Neuronal Endosomes to Lysosomes: A Journey to the Soma. *J. Cell Biol.* 2018, 217, 2977–2979, doi:10.1083/jcb.201806139.
21. 21. Kim, S.-I.; Yi, J.-S.; Ko, Y.-G. Amyloid  $\beta$  Oligomerization Is Induced by Brain Lipid Rafts. *J. Cell. Biochem.* 2006, 99, 878–889, doi:https://doi.org/10.1002/jcb.20978.
22. 22. Xia, Z.; Liu, Y. Reliable and Global Measurement of Fluorescence Resonance Energy Transfer Using Fluorescence Microscopes. *Biophys. J.* 2001, 81, 2395–2402.
23. 23. Su, Y.; Chang, P.-T. Acidic PH Promotes the Formation of Toxic Fibrils from  $\beta$ -Amyloid Peptide. *Brain Res.* 2001, 893, 287–291, doi:10.1016/S0006-8993(00)03322-9.
24. 24. Jarrett, J.T.; Berger, E.P.; Lansbury, P.T. The Carboxy Terminus of the .Beta. Amyloid Protein Is Critical for the Seeding of Amyloid Formation: Implications for the Pathogenesis of Alzheimer's Disease. *Biochemistry* 1993, 32, 4693–4697, doi:10.1021/bi00069a001.
25. 25. Asami-Odaka, A.; Ishibashi, Y.; Kikuchi, T.; Kitada, C.; Suzuki, N. Long Amyloid Beta-Protein Secreted from Wild-Type Human Neuroblastoma IMR-32 Cells. *Biochemistry* 1995, 34, 10272–10278, doi:10.1021/bi00032a022.
26. 26. Yu, Y.; Jans, D.C.; Winblad, B.; Tjernberg, L.O.; Schedin-Weiss, S. Neuronal A $\beta$ 42 Is Enriched in Small Vesicles at the Presynaptic Side of Synapses. *Life Sci. Alliance* 2018, 1, doi:10.26508/lsa.201800028.
27. 27. Feige, J.N.; Sage, D.; Wahli, W.; Desvergne, B.; Gelman, L. PixFRET, an ImageJ Plug-in for FRET Calculation That Can Accommodate Variations in Spectral Bleed-Throughs. *Microsc. Res. Tech.* 2005, 68, 51–58, doi:https://doi.org/10.1002/jemt.20215.